

Identification of an "Exceptional Responder" Cell Line to MEK1 Inhibition: Clinical Implications for MEK-Targeted Therapy

Hugh S. Gannon^{1,2}, Nathan Kaplan^{1,2}, Aviad Tsherniak¹, Francisca Vazquez^{1,2}, Barbara A. Weir^{1,2}, William C. Hahn^{1,2,3,4}, and Matthew Meyerson^{1,2,3,5}

Abstract

The identification of somatic genetic alterations that confer sensitivity to pharmacologic inhibitors has led to new cancer therapies. To identify mutations that confer an exceptional dependency, shRNA-based loss-of-function data were analyzed from a dataset of numerous cell lines to reveal genes that are essential in a small subset of cancer cell lines. Once these cell lines were determined, detailed genomic characterization from these cell lines was utilized to ascertain the genomic aberrations that led to this extreme dependency. This method, in a large subset of lung cancer cell lines, yielded a single lung adenocarcinoma cell line, NCI-H1437, which is sensitive to RNA interference of MAP2K1 expression. Notably, NCI-H1437 is the only lung cancer cell line included in the dataset with a known activating mutation in MAP2K1 (Q56P). Subsequent validation using shRNA and CRISPR-Cas9 confirmed MAP2K1 dependency. *In vitro* and *in vivo* inhibitor studies established that NCI-H1437 cells are sensitive to

MEK1 inhibitors, including the FDA-approved drug trametinib. Like NCI-H1437 cells, the MAP2K1-mutant cell lines SNU-C1 (colon) and OCUM-1 (gastric) showed decreased viability after MAP2K1 depletion via Cas9-mediated gene editing. Similarly, these cell lines were particularly sensitive to trametinib treatment compared with control cell lines. On the basis of these data, cancers that harbor driver mutations in MAP2K1 could benefit from treatment with MEK1 inhibitors. Furthermore, this functional data mining approach provides a general method to experimentally test genomic features that confer dependence in tumors.

Implications: Cancers with an activated RAS/MAPK pathway driven by oncogenic MAP2K1 mutations may be particularly sensitive to MEK1 inhibitor treatments. *Mol Cancer Res*; 14(2): 207–15. ©2015 AACR.

Introduction

Targeted therapies have revolutionized cancer gene discovery and drug development. Unlike conventional cancer treatments such as radiation and general chemotherapy, targeted therapies seek to inhibit somatically mutated or dysregulated genes found preferentially in cancer cells. For example, the drug imatinib inhibits the essential *BCR-ABL1* gene fusion found in most chronic myelogenous leukemia patients, and estrogen receptor (ER) inhibitors benefit patients with ER-positive luminal breast cancer (1, 2). These discoveries have influenced cancer researchers to identify essential driver oncogenes that could lead to targeted drug development efforts in specific tumor types.

Retrospective data from clinical trials allow a converse strategy that couples effective targeted therapies to specific cancer muta-

tions by sequencing tumors of the few cancer patients that show a positive response to a drug that fails to have an effect on the majority of patients in the trial (3). Identifying a common mutant gene in these patients may reveal the cancer-specific target that is affected by the drug. Such "exceptional responder" patient studies have identified sensitivity to the drug everolimus in bladder cancers harboring *TSC1* mutations and revealed mutant *ARAF* as a potential target in a patient with an outlier response to the drug sorafenib (3–5). Although relatively rare, these N-of-1 studies are a powerful resource for identifying specific genetic events that allow certain drugs to be effective in actual cancer patients, information that is elusive for many cancer drugs.

The advent of next-generation sequencing has facilitated the genomic characterization of tumors of patients and enabled large-scale functional genomic analyses *in vitro*. The Cancer Cell Line Encyclopedia (CCLE, <http://www.broadinstitute.org/ccle>) and Sanger Cell Lines Project (cancer.sanger.ac.uk) have created publicly accessible databases documenting genomic alterations in hundreds of cancer cell lines (6, 7). These data can potentially be paired with genome-scale functional genomic screens of essentiality to match genetic dependencies with mutations or gene expression patterns. One such genome-scale shRNA screen performed in 216 cancer cell lines across a variety of lineages is publicly available (www.broadinstitute.org/achilles; ref. 8). The uniquely large number and variety of cell lines screened allows for comparison of survival differences in different genetic contexts after knockdown of individual genes, leading to hypotheses generation and subsequent preclinical validation.

¹Broad Institute of Harvard and MIT, Cambridge, Massachusetts.

²Department of Medical Oncology, Dana-Farber Cancer Institute, Boston, Massachusetts. ³Center for Cancer Genome Discovery, Dana-Farber Cancer Institute, Boston, Massachusetts. ⁴Departments of Medicine, Brigham and Women's Hospital, Harvard Medical School, Boston, Massachusetts. ⁵Department of Pathology, Harvard Medical School, Boston, Massachusetts.

Note: Supplementary data for this article are available at Molecular Cancer Research Online (<http://mcr.aacrjournals.org/>).

Corresponding Author: Matthew Meyerson, Dana-Farber Cancer Institute, 450 Brookline Ave., Boston, MA 02215. Phone: 617-632-4768; Fax: 617-582-7880; E-mail: matthew_meyerson@dfci.harvard.edu

doi: 10.1158/1541-7786.MCR-15-0321

©2015 American Association for Cancer Research.

Gannon et al.

To mirror "exceptional responder" studies *in vitro*, we mined cell line RNAi and genomic datasets to identify genes upon which a small number of cell lines are uniquely dependent (6–8). We focused on the 21 lung cancer lines tested by shRNA analysis. Knockdown and genomic data for these cell lines were then mined to link extreme dependencies to genetic features.

Materials and Methods

Data mining and analysis

Cancer cell line sequencing data were acquired from the public CCLE and Sanger Cell Line data portals. The shRNA-level data for Project Achilles version 2.4.3 are available at <http://www.broadinstitute.org/achilles/datasets/all> (8). shRNA level dependency values are expressed as the log₂ fold change in shRNA abundance after 16 population doublings or 40 days in culture compared with the initial DNA plasmid pool. To calculate gene-level scores for all genes included in this dataset, we used the ATARiS module on GenePattern (<http://www.broadinstitute.org/cancer/ataris>) using a null significance value of 1 (9). The gene-level score is a normalized value indicating the magnitude of dependence (negative score) or relative enhancement (positive score) of survival after shRNA knockdown.

Cancer cell lines

Cancer cell lines were grown and maintained in RPMI media supplemented with 10% FBS, penicillin, streptomycin, and L-glutamine. The following lung cancer cell lines were originally provided by the laboratory of Dr. John Minna (Hamon Center for Therapeutic Oncology Research at UT Southwestern Medical Center): NCI-H1437, A549, NCI-H460, NCI-H1299, NCI-H1650, HCC366, and NCI-H2126. The following cancer cell lines were provided by the CCLE: SW1573, NCI-H1355, NCI-H196, and NCI-H226 (lung); SNU-C1, RKO, SW48, HCT116, and NCI-H508 (colorectal); OCUM-1, AGS, MKN7, and NCI-N87 (stomach).

Immunoblots

Cells were lysed in RIPA lysis buffer (Thermo Scientific) supplemented with 1× protease and phosphatase inhibitor cocktails (Roche). Protein extracts were analyzed by standard immunoblotting with the following antibodies: total MEK1/2 (9122), phospho-ERK Y202/Y204 D13.14.4E (4370), total ERK 3A7 (9107), phospho-AKT S473 193H12 (4058), and total AKT 2H10 (2967) from Cell Signaling Technology; β-actin C4 (sc-47778) from Santa Cruz Biotechnology.

Inhibitor treatment analysis

For drug treatment assays, cells were plated at a density of 2,500 cells per well in a 96-well assay plate. The following day, cells were treated with the corresponding MEK1 inhibitors: selumetinib (AZD6244) S1008, trametinib (GSK1120212) S2673, and PD0325901 S1036 from Selleck Chemicals and refametinib (RDEA119) from ChemieTek. Control wells were treated with DMSO. Cell viability was assayed 6 days after drug treatment with CellTiter-Glo Luminescent Cell Viability Assay kit (Promega). Viability was normalized to DMSO controls. IC₅₀ estimates were obtained using least-squares nonlinear regression on a standard four-parameter logistic model.

Lentiviral-delivered shRNA

The following sequences targeting *GFP*, *LacZ*, and *MAP2K1* were obtained from The RNAi Consortium (TRC) portal (<http://www.broadinstitute.org/mai/public>) and cloned into the lentiviral vector pLKO.1:

GFP shRNA ACAACAGCCACAACGTCTATA
LacZ shRNA CGACCACGCAAATCAGCGATT
MAP2K1 shRNA-1 GCTTCTATGGTGCCTTCTACA
MAP2K1 shRNA-2 GAGGGAGAAGCACAAGATCAT

For virus production, each pLKO.1 vector and packaging vectors were introduced into 293T cells via calcium phosphate transfection (Clontech). Lentivirus was harvested in RPMI media supplemented with 10% FBS and filtered before addition to each cancer cell line. Infected cells were selected in 2 μg/mL puromycin for 5 days and harvested for protein lysates or for proliferation assays in 96-well plates and grown in the presence of RPMI containing 10% FBS and 1 μg/mL puromycin. Cell viability was assayed after 6 days using the CellTiter-Glo Luminescent Cell Viability Assay Kit (Promega).

The following guide RNA sequences targeting *MAP2K1* were designed using the sgRNA Designer tool on TRC portal (<http://www.broadinstitute.org/mai/public/analysis-tools/sgrna-design>):

CRISPR-Cas9 lentiviral deletions

The following guide RNA sequences targeting *MAP2K1* were designed using the sgRNA Designer tool on TRC portal (<http://www.broadinstitute.org/mai/public/analysis-tools/sgrna-design>):

MAP2K1 sgRNA-1 ACATCCTAGTCAACTCCCGT (sgRNA score = 0.70)
MAP2K1 sgRNA-2 GCTGATGTTTGGGTGCCAGG (sgRNA score = 0.70)

The sgRNA sequences targeting *GFP* were described previously (10):

GFP sgRNA-1 GGAGCGCACCATCTTCTTCA
GFP sgRNA-2 GAAGTTCGAGGGCGACACCC

These sequences were cloned into the Cas9-expressing lentiviral vector CRISPRv2 (11). Virus production, infection, and selection procedures were as described for shRNA experiments. Immunoblotting confirmed decreased MEK1 protein levels across the pool of infected cells. Cell viability was assayed 3 and 6 days later with the CellTiter-Glo Luminescent Cell Viability Assay kit (Promega).

Xenografts

Xenografts were performed as previously described (12). Two hundred microliters of each cell line suspended in Matrigel were injected into each of two injection sites in the flank of 4-week-old female nu/nu mice (The Jackson Laboratory). Tumor volume was measured with a digital caliper twice weekly and calculated using the formula $0.5 \times L \times W^2$, where *L* is the longest diameter and *W* is the diameter perpendicular to *L*. Drug treatments began once established tumors grew to 200 mm³ total volume. Trametinib was suspended in 5% DMSO and a dose of 0.3 mg/kg was administered daily by oral gavage. Control mice were treated with 5% DMSO. All animal experiments were carried out in accordance with the Dana-Farber Cancer Institute Institutional Animal Care and Use Committee guidelines.

Results

To explore associations between potential drug targets and specific genomic features, we mined genome-scale shRNA-

mediated loss-of-function data from Project Achilles. This large-scale project targeted 11,194 genes with 54,020 shRNAs in 216 human cancer cell lines, and the depletion or enrichment of specific shRNAs was measured after cells were grown *in vitro* for several weeks (8). The use of five shRNAs per gene and the large number of cell lines permits one to identify shRNAs that show similar phenotypic patterns to reduce the contribution of off-target effects. ATARiS is a computational method that uses this information to compute a gene-level dependency score (9).

We first explored known relationships between the dependencies and genomic features seen in current targeted therapies. One example discussed above is the inhibition of cells harboring the *BCR-ABL1* translocation by the tyrosine kinase inhibitor, imatinib. To evaluate genetic dependency in such cells, we assessed the impact of *ABL1* knockdown in the 30 hematopoietic and lymphoid cell lines included in the dataset. Of these lines, the three known to harbor the *BCR-ABL1* translocation are the most sensitive to *ABL1* knockdown (Fig. 1A). The large difference in the scores between these three cell lines compared with the *BCR-ABL1*-negative cell line with the lowest score (LAMA84 = 1.4; K562 = 1.0; and HNT34 = 0.63) indicates an outlier dependency pattern. This was seen using both ATARiS gene solutions generated from the screen (Supplementary Fig. S1; ref. 9). We found a

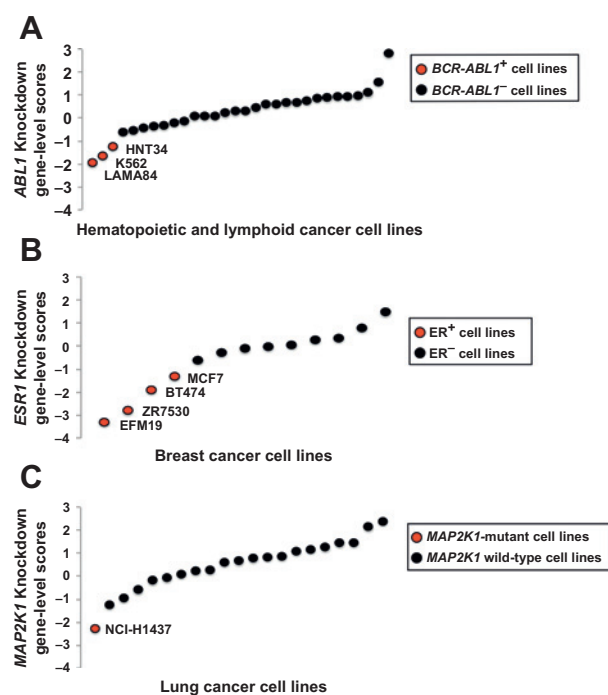


Figure 1.

A, each data point represents the normalized gene-level dependency scores for *ABL1* calculated using ATARiS (gene solution 1) in the 30 hematopoietic and lymphoid cell lines tested (8). The three most sensitive cell lines (indicated by red circles) are the only lines within this dataset known to harbor the *BCR-ABL1* translocation. B, each data point represents the normalized gene-level dependency scores for *ESR1* in the 13 breast cancer cell lines tested (8). The four most sensitive cell lines (indicated by red circles) are the only breast cancer cell lines within this dataset known to be positive for the ER. C, each data point represents the normalized gene-level dependency scores for *MAP2K1* in the 21 lung cancer cell lines tested (8). The most sensitive cell line (indicated by the red circle) is the only lung cancer cell line within this dataset known to harbor a *MAP2K1* mutation.

similar pattern across the 13 breast cancer cell lines profiled, as the 4 ER-positive cell lines were the most sensitive to *ESR1* knockdown, which parallels antiestrogen treatments in patients with ER-positive breast tumors (Fig. 1B). These observations demonstrate that relationships between strong dependencies and genomic features could be detected in this RNAi dataset.

To perform an unbiased search for outlier dependencies in lung cancer cell lines, we ordered all genes in the 21 lung cancer cell lines included in the dataset by the dependency score. We then calculated an outlier score: the difference in gene-level scores between the cell line with the lowest score and the cell line with the gene-level score at the 90th percentile. Once we generated a ranked list of outlier scores across the lung cancer cell lines, we searched for genes with the highest outlier scores that were also significantly mutated in lung cancers to identify genes whose exceptional dependency may be due to known oncogenic drivers in lung cancers. Of the known oncogenic drivers in lung cancers, *MAP2K1* showed the highest outlier score (1.7, top 1% of outlier scores; Fig. 1C). The *MAP2K1* gene encodes the protein kinase MEK1, known to be a part of the oncogenic RAS/MAPK pathway. This prosurvival and proliferative pathway is commonly activated by oncogenic mutations in many tumor types including lung adenocarcinoma (13–16). The importance of this pathway is highlighted by many established and ongoing drug discovery efforts to inhibit different nodes in this signaling pathway such as mutant EGFR, mutant KRAS, mutant BRAF, and downstream wild-type MEK1.

MEK1 acts downstream from more commonly mutated RAS/MAPK pathway members including KRAS, EGFR, BRAF, RIT1, MET, and ERBB2 (16). *MAP2K1* mutations occur at a significant but low frequency in lung adenocarcinoma (<1%; refs. 13–15, 17), and *MAP2K1* mutations have been observed and characterized in melanoma (18), gastric cancer (19), Langerhans cell histiocytosis (20, 21), and hairy-cell leukemia (22). Notably, a recent comprehensive study of *MAP2K1* somatic mutations in lung adenocarcinoma reveals that about 86% of the *MAP2K1* mutations are clustered between amino acid residues 53–57 in exon 2, which encodes a critical α -helix domain (13). The recurrence and concentration of these mutations in this region indicate functional significance, and mutations in this region are predicted to affect MEK1 kinase activity. This study also demonstrated that overexpression of MEK1 proteins with mutations in this region, including F53L, Q56P, and K57N, leads to downstream ERK phosphorylation and increased colony formation that is inhibited with the MEK1/2 inhibitor, selumetinib (AZD6244; ref. 13). In addition, large-scale genomic characterizations of lung adenocarcinomas found that *MAP2K1* mutations in this region do not cooccur with oncogenic mutations in receptor tyrosine kinases or RAS/MAPK pathway members, suggesting that oncogenic mutant *MAP2K1* drives RAS/MAPK pathway activation in these cases (14, 15). Interestingly, two lung adenocarcinomas that harbor atypical *MAP2K1* mutations, M146I and S331R, also bear activating *KRAS* mutations, suggesting that these uncharacterized *MAP2K1* mutations may not be potent oncogenic driver mutations (13, 14).

Plotting the gene-level dependency scores for *MAP2K1* shows the most sensitive cell line, NCI-H1437, as a potential outlier compared with the rest of the lung cancer cell lines tested, with a relatively high outlier score (1.7) in our analysis (Fig. 1C). Interestingly, NCI-H1437 is the only lung cancer cell line included

Gannon et al.

in the dataset that has a *MAP2K1* mutation (Q56P). Consistent with the mutant *MAP2K1* lung adenocarcinoma cases in the study described above, sequencing analyses show no other oncogenic driver mutations of the RAS/MAPK pathway in the NCI-H1437 line (13).

To confirm *MAP2K1* dependence in NCI-H1437 cells, we used two shRNAs targeting *MAP2K1* and two shRNA controls. The *MAP2K1* shRNAs effectively decreased MEK1 protein levels (Fig. 2A). *MAP2K1* knockdown resulted in decreased viability in the NCI-H1437 cells but not in A549 cells, which harbor an activating *KRAS* mutation (G12S; Fig. 2B). Consistent with our results, the *MAP2K1* dependency score for A549 cells indicates no effect (gene-level score = -0.2).

To confirm these observations, we used CRISPR-Cas9 gene-editing technology to deplete *MAP2K1* (10). Pooled populations of cells were assayed after lentiviral infection with Cas9 and a small guide RNA (sgRNA) targeting either *GFP* or *MAP2K1*. Introduction of both *MAP2K1*-targeting sgRNAs resulted in decreased MEK1 protein expression in NCI-H1437 and A549 cells (Fig. 2C). Similar to the shRNA knockdown experiments, *MAP2K1* knockout resulted in decreased cell viability in NCI-H1437 cells, whereas A549 cells were unaffected (Fig. 2D). These results confirmed the strong dependency on *MAP2K1* expression in NCI-H1437 cells.

Our analysis and validation experiments suggest that NCI-H1437 cells would also show increased sensitivity to MEK1 inhibition using a small molecule. To test this, we performed dose response curves in a variety of lung cancer cell lines treated with MEK1/MEK2 inhibitors. We included the only other lung cancer cell line that harbors a *MAP2K1* mutation: NCI-H460 cells have an atypical *MAP2K1* Y134C substitution and also have an activating *KRAS* mutation (Q61H). This cell line was not included in the 216-cell line gene knockdown dataset.

A previous study demonstrated that NCI-H1437 cells are sensitive to selumetinib, a MEK1/MEK2 inhibitor (23). In agreement with this result and our genetic knockdown and gene-knockout data, we found that NCI-H1437 cells were sensitive to selumetinib treatment, with an IC_{50} value in the nanomolar range, approximately 10-fold less than the maximal serum concentration achieved in patients with the recommended dose from phase I trials (Fig. 3A, dashed line; ref. 24). Strikingly, NCI-H1437 cells showed sensitivity in the picomolar range upon treatment of the FDA-approved MEK1/MEK2-targeting drug, trametinib (GSK1120212), with an estimated IC_{50} value 1,000-fold lower than the IC_{50} values from a panel of similarly treated lung cancer cell lines (Fig. 3B; Supplementary Fig. S2A). This dose was also over 100-fold less than the maximal serum concentration achieved in patients treated with the recommended dose of

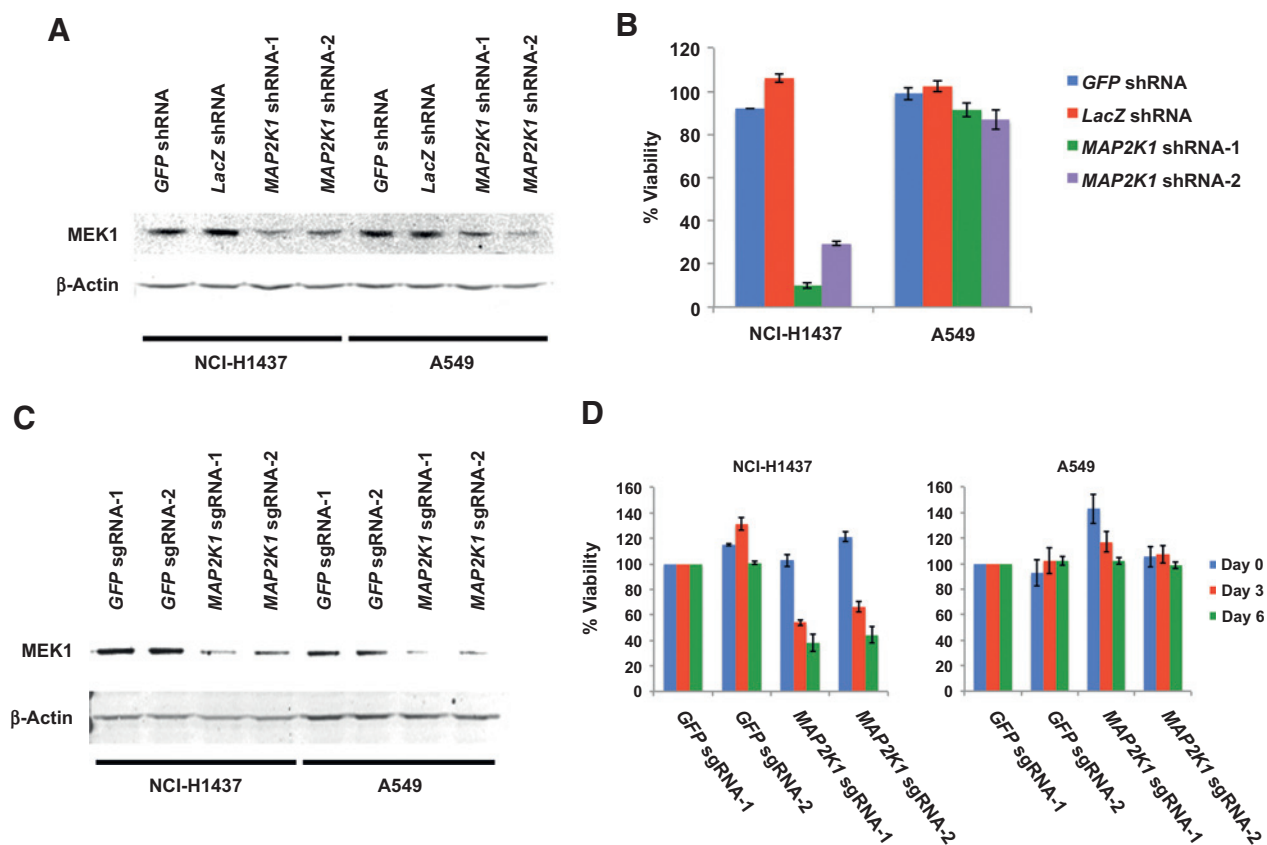
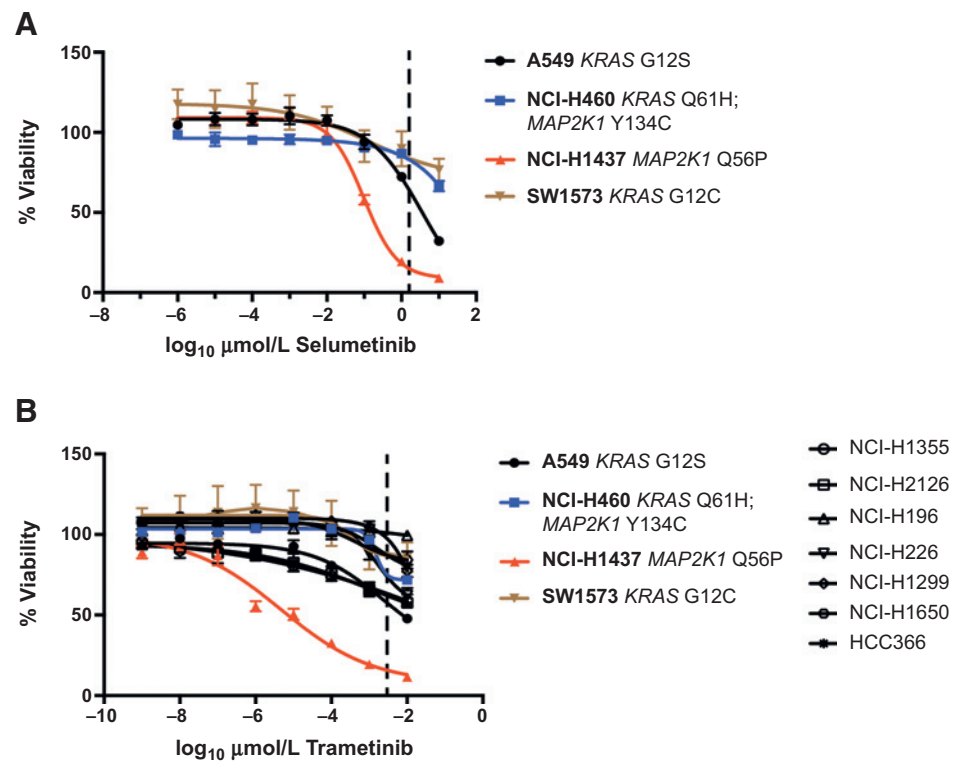


Figure 2.

A, immunoblot of MEK1 and β -actin (loading control) protein levels 5 days after lentiviral infection of control shRNAs (*GFP* and *LacZ*) and two independent *MAP2K1* shRNAs in NCI-H1437 and A549 cells. B, cell viability beginning 7 days after lentiviral infections. Viability is normalized to mock-infected controls. C, immunoblot of MEK1 and β -actin (loading control) protein levels from pooled population of cells 5 days after lentiviral infection of Cas9 with two independent control sgRNAs, each targeting either *GFP* or *MAP2K1* in NCI-H1437 and A549 cells. D, cell viability beginning 7 days after Cas9/sgRNA infections. Viability is normalized to control *GFP* sgRNA-1 for each cell line on each day.

Figure 3.

A, selumetinib dose-response curve after 6 days. Cell viability was normalized to DMSO-treated controls. The dashed line approximately represents the maximal serum concentration achieved in phase I clinical trials (24). B, trametinib dose response curve after 6 days. Cell viability normalized to DMSO-treated controls. The dashed line approximately represents the serum concentration achieved from the recommended dose determined from phase I clinical trials (25).



trametinib from phase I trials (Fig. 3B, dashed line; ref. 25). We also tested additional MEK1 inhibitors, refametinib (RDEA119) and PD0325901, and again found that NCI-H1437 cells were the most sensitive to both drugs, although the difference in sensitivity compared with other cell lines was less pronounced than with trametinib treatment (Supplementary Fig. S2B). These results further underscore the acute dependence of NCI-H1437 cells on functional MEK1.

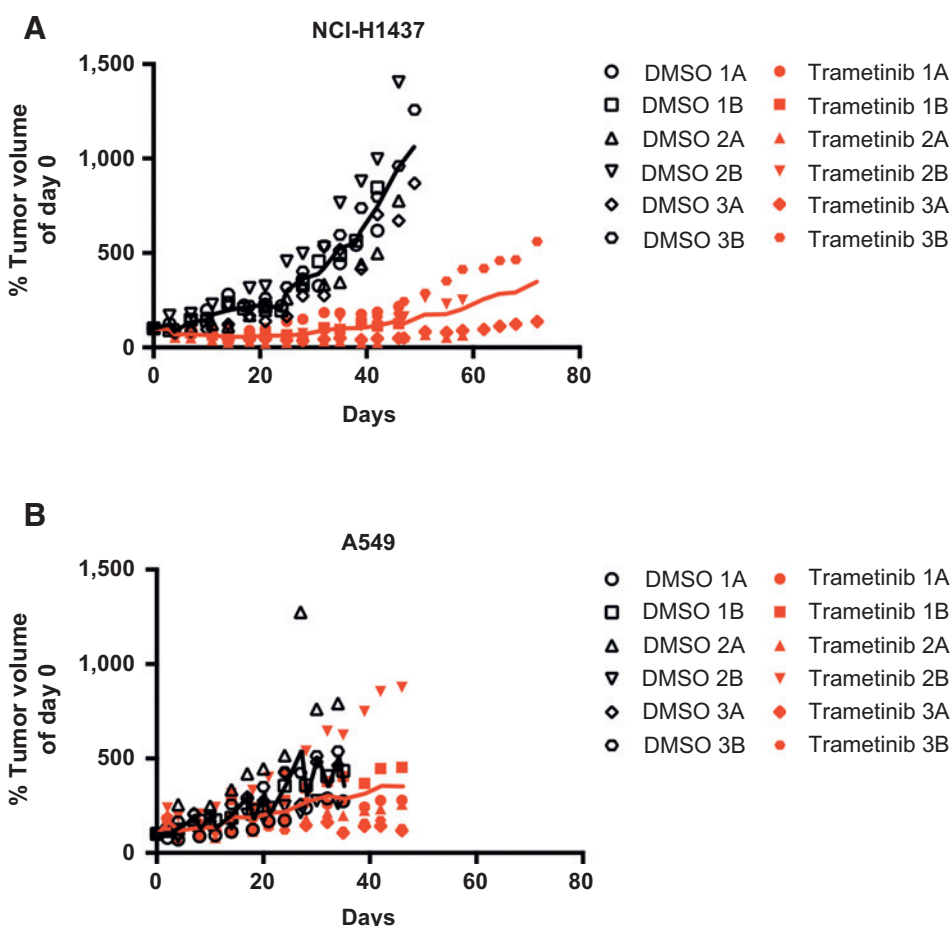
While MEK1 inhibition strongly suppressed growth of NCI-H1437 cells, the only other lung line with a *MAP2K1* mutation, NCI-H460, was not as affected. The *MAP2K1* mutation in NCI-H460 cells (Y134C) has not been reported in any cancer study or additional cell line to date, and is not functionally characterized. In addition, NCI-H460 cells have an activating *KRAS* mutation (Q61H). Thus, the *KRAS* mutation or other activated oncogenic pathways in NCI-H460 cells may favor cell survival even in the presence of MEK1 inhibitors. We treated lung cancer cell lines with trametinib and assayed the effect on the *KRAS* signaling pathway. Trametinib resulted in a clear decrease in phosphorylated ERK levels in all cells tested; however, only the NCI-H1437 cells lacked detectable phosphorylated AKT, and trametinib treatment had no effect on the elevated phosphorylated AKT in the *KRAS*-mutant lines A549, NCI-H460, and SW1573 (Supplementary Fig. S2C). The lack of compensatory signaling by phosphorylated AKT in NCI-H1437 cells may help to explain the exquisite sensitivity of this cell line to MEK1 inhibition.

The drug trametinib displayed potent effects preferentially in the NCI-H1437 cells compared with all the other lung cell lines assayed. To validate this *in vivo*, we performed trametinib drug treatments in mice bearing NCI-H1437 and A549-derived xenografts. Once tumors were established, we treated the mice daily

with 0.3 mg/kg trametinib or vehicle. While control (DMSO-treated) NCI-H1437 tumors grew readily, tumors of mice treated with trametinib showed little to no growth for the duration of the experiment (Fig. 4A). This was repeated in an independent experiment, which gave similar results (Supplementary Fig. S3). In comparison, A549 tumors grew regardless of drug treatment (Fig. 4B). Of note, all A549 mice and control NCI-H1437 mice were sacrificed due to excessive tumor burden.

Our analysis of *MAP2K1* dependence and activating *MAP2K1* driver mutations specifically in lung cancer cell lines is limited to NCI-H1437 cells, as this is the only lung cancer cell line with an activating *MAP2K1* mutation to our knowledge. Therefore, we tested additional mutant *MAP2K1* cell lines from different lineages to expand our study and determine whether the relationship between mutant *MAP2K1* and sensitivity to MEK1 inhibition is observed across different cancer types. This is particularly important as many emerging umbrella trials, such as the NCI-MATCH trials, pair targeted therapies to patients with tumors harboring specific oncogenic mutations regardless of tumor type (26). Our search produced no cancer cell lines that harbor a *MAP2K1* K57N mutation, the most frequently observed *MAP2K1* mutation in lung adenocarcinoma that lies within the inhibitory α -helical domain of MEK1 (13). However, we did find two cancer cell lines with activating mutations in *MAP2K1* within this region as the sole oncogenic driver of the RAS/MAPK pathway. The first of these is SNU-C1, a colorectal cancer cell line that has an F53L *MAP2K1* substitution. This line is also included in the Project Achilles knockdown dataset and displayed the lowest dependence score to *MAP2K1* knockdown (-2.9) of any of the 216 cell lines assayed. To validate this dependency, we used CRISPR-Cas9 gene editing to decrease MEK1 levels in a control colorectal cell line, RKO (*MAP2K1* knockdown dependence score = -0.2), and SNU-

Gannon et al.

**Figure 4.**

A, xenograft tumor growth after NCI-H1437 subcutaneous injection in nude mice. Mice were treated daily with either vehicle (5% DMSO) or 0.3 mg/kg trametinib. Each number represents a single mouse and the letters A and B represent each tumor. Tumor volume was normalized to its size at the start of drug treatment. Solid lines indicate the average of the six tumors for each treatment. The differences between trametinib and control treatments for all days after day 8 were statistically significant ($P < 0.007$). Control mice were all sacrificed during the experiment due to excessive tumor burden. All trametinib-treated mice were sacrificed at the conclusion of the experiment. B, xenograft tumor growth after A549 subcutaneous injection in nude mice. Mice were treated daily with either vehicle (5% DMSO) or 0.3 mg/kg trametinib. For each tumor, the volume was normalized to the size at the start of drug treatment. Control and trametinib treated mice were all sacrificed during the experiment due to excessive tumor burden.

C1 cells (Fig. 5A). While the RKO cells were insensitive to *MAP2K1* knockout, SNU-C1 viability was diminished, confirming what was observed in the original pooled screen (8). Treatment of different colorectal cancer cell lines with trametinib revealed strong sensitivity in the SNU-C1 cells, similar to what we observed in trametinib-treated NCI-H1437 cells (Fig. 5C).

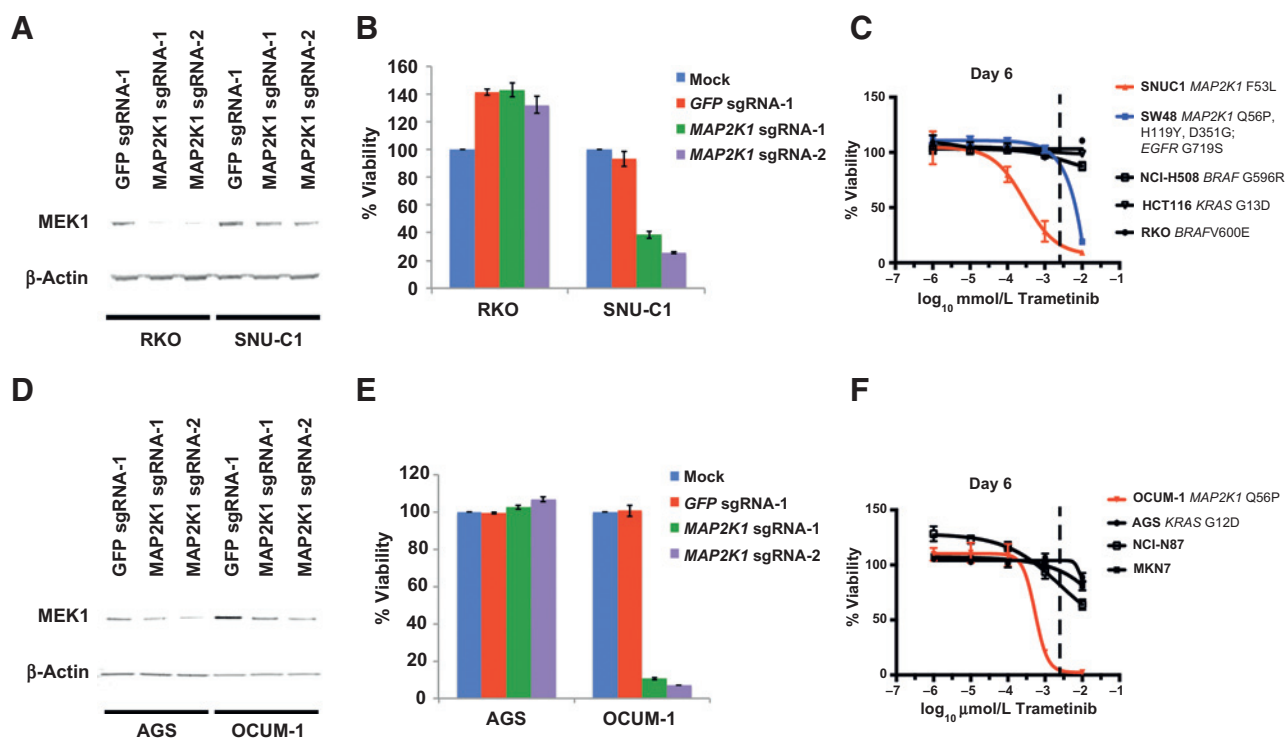
In addition to the SNU-C1 and control colorectal cell lines with *BRAF* or *KRAS* mutations, we also tested the sensitivity of SW48 cells to trametinib treatment. SW48 is a colorectal cancer cell line with three detected mutations in *MAP2K1* (Q56P, H119Y, and D351G), as well as an activating mutation in *EGFR* (G719S). Our laboratory previously characterized the dependency of this cell line on EGFR signaling using the EGFR inhibitor cetuximab both *in vitro* and in xenografts (27). SW48 cells were also included in Project Achilles, resulting in a moderate dependence score to *MAP2K1* knockdown (-0.3). SW48 cells displayed increased sensitivity to trametinib compared with control cell lines but not to the same degree of SNU-C1 cells (Fig. 5C). As activating *MAP2K1* mutations in cancer patient samples are almost always mutually exclusive with other mutations of the RAS/MAPK pathway, the SW48 cells present an atypical case where activated EGFR signaling may compensate for MEK1 inhibition.

The only other cell line identified to date with a mutation within the inhibitory α -helix of *MAP2K1* is the gastric cancer cell line OCUM-1 (Q56P). Like NCI-H1437 and SNU-C1 cells, mutant *MAP2K1* was the only RAS/MAPK pathway driver muta-

tion in OCUM-1 cells. A previous report describing *MAP2K1* mutations in epithelial tumors determined that OCUM-1 cells were sensitive to selumetinib treatment compared with two wild-type *MAP2K1* gastric cancer cell lines (19). To further confirm this, we used CRISPR-Cas9-mediated gene editing to deplete MEK1 levels in pools of infected OCUM-1 and the control gastric cancer cell line AGS (Fig. 5D). This resulted in greatly decreased viability in the OCUM-1 cells but not in the AGS cells (Fig. 5E). Importantly, we tested the sensitivity of OCUM-1 and three other gastric cancer cell lines with wild-type *MAP2K1* to trametinib treatment (Fig. 5F). OCUM-1 cells were sensitive to picomolar concentrations of trametinib, similar to what we observed in the NCI-H1437 and SNU-C1 cells. These results further support outlier dependencies in cell lines with mutant *MAP2K1*-driven RAS/MAPK pathway activation to MEK1 inhibition.

Discussion

To reveal potential associations between cancer cell line features and dependencies, we mined existing large-scale functional genomic datasets. This approach allowed us to search for potential "exceptional responder" lung cancer cell lines to discover specific drug targets. We believe this approach is a simple, unbiased method that can identify robust dependencies in a subset of cell lines from large cell line cohorts tested in these knockdown experiments. Furthermore, while inherent, powerful off-target effects of shRNAs can lead to false results, our analysis should

**Figure 5.**

A, immunoblot of MEK1 and β -Actin (loading control) protein levels from pooled population of cells 5 days after lentiviral infection of Cas9 with control sgRNA targeting *GFP* or two independent sgRNAs targeting *MAP2K1* in RKO and SNU-C1 cells. B, cell viability beginning 7 days after Cas9/sgRNA infections. Viability is normalized to mock-infected controls for each cell line. C, trametinib dose-response curve after 6 days. Cell viability normalized to DMSO-treated controls. The dashed line approximately represents the serum concentration achieved from the recommended dose determined from phase I clinical trials (25). D, immunoblot of MEK1 and β -actin (loading control) protein levels from pooled population of cells 5 days after lentiviral infection of Cas9 with control sgRNA-targeting *GFP* or two independent sgRNAs targeting *MAP2K1* in AGS and OCUM-1 cells. E, cell viability beginning 7 days after Cas9/sgRNA infections. Viability is normalized to mock-infected controls for each cell line. F, trametinib dose-response curve after 6 days. Cell viability normalized to DMSO-treated controls. The dashed line approximately represents the serum concentration achieved from the recommended dose determined from phase I clinical trials (25).

reliably identify very strong cancer dependencies that can be further validated.

Our analysis revealed that knockdown of *MAP2K1*, significantly mutated in lung adenocarcinoma, resulted in an outlier phenotype in a single cell line, NCI-H1437, in the original dataset, (8, 13–15, 17). Importantly, this is the only lung cell line in this dataset with a *MAP2K1* mutation, the previously established activating Q56P substitution (13). As different MEK1 inhibitors such as trametinib, which was recently approved to treat mutant BRAF-driven tumors in melanoma patients, and selumetinib are being tested in clinical trials for lung cancer patients, our study indicates that these drug treatments may be the most beneficial in the small but significant percentage of patients whose tumors harbor activating *MAP2K1* mutations.

A previous study, characterizing the first reported *MAP2K1* mutations in lung cancer, demonstrated that NCI-H1437 cells were sensitive to MEK1 inhibition by selumetinib (23). This study stated that NCI-H1437 cells displayed sensitivity to selumetinib in the nanomolar range. Our results support this work and provide independent evidence of the exceptional dependency of NCI-H1437 cells on MEK1-driven signaling *in vitro*. In addition, we observed a dramatic reduction in growth of NCI-H1437 tumor xenografts upon treatment with specific MEK1 inhibitors. Our initial data analysis proposing this dependence was also in the context of 21 different lung cancer

cell lines, further corroborating the hypothesis that *MAP2K1*-mutant cells and cancers may be extremely sensitive to MEK1 inhibitors, particularly trametinib (28).

MEK1 inhibitors were developed to block aberrant RAS/MAPK signaling in cancer. Because MEK1 lies downstream in this pathway, MEK1 inhibitors are thought to indirectly suppress activating oncogenes that lie upstream in this signaling cascade, such as mutant KRAS (28). While shRNA knockdown screen data do not always correlate with drug efficacy in patients, it is interesting to note that sensitivity to *MAP2K1* knockdown did not correlate with KRAS mutation or any other oncogenic driver mutations across the lung cell line cohort except mutant *MAP2K1* (Supplementary Table S1). However, it is important to note that many small molecules that target MEK1 also target MEK2, while *MAP2K1*-targeting shRNAs should not affect *MAP2K2* expression.

Our work further highlights the need to identify the oncogenic drivers that are present in each cancer patient. Efforts for systematic hybrid capture sequencing can identify patients with *MAP2K1*-activating mutations that do not occur with other known driver oncogene mutations (29, 30). On the basis of our results, these patients may benefit the most from trametinib treatment. In addition, an activating *MAP2K1* mutation was recently described as the potential basis for resistance to treatment with ceritinib in an ALK-positive tumor (31). Therefore, sequence knowledge at different stages of tumor evolution in response to

drug treatment might suggest combination treatments with MEK1 inhibitors should *MAP2K1* mutations be detected. Lung adenocarcinoma is one of the deadliest cancer types, and overall survival of *MAP2K1*-mutant lung adenocarcinoma patients has been shown to be decreased compared with patients with other oncogene-driven tumors (13). Therefore, matching *MAP2K1*-mutant lung cancer patients to MEK1 inhibitor treatments will be important and is clinically achievable.

Identifying specific oncogenic driver mutations in patients will also be critical in the design and retrospective analysis of clinical trials assessing MEK1 inhibition in different tumor types. Because of the low frequency of *MAP2K1* mutations, those few patients with these oncogenic alterations might be neglected in trials comparing other factors, for example, *KRAS* wild-type and *KRAS*-mutant tumors. On the basis of our results and the current literature, it will be important to identify and include patients with mutant *MAP2K1* in clinical trials for MEK1 inhibition. Multi-institutional clinical trials that include a larger number of patients with *MAP2K1*-mutant cancers might be needed to truly assess MEK1 inhibitor efficacy in this population. Likewise, previously conducted trials that included appropriate sequencing data could uncover responses in mutant *MAP2K1* patients. Excitingly, a very recent study of an ovarian cancer patient with a long-term, complete response to selumetinib treatment revealed a novel somatic 15 base pair deletion of the inhibitory α -helix domain in *MAP2K1* (32). This independent evidence further supports the findings of this work and the need for further clinical testing of MEK1 inhibitors in patients harboring activating *MAP2K1* mutations.

As functional genomic screens continue to evolve, greater numbers of hypotheses regarding putative drug targets can be generated and tested. Emerging technologies using CRISPR-mediated gene editing allow specific and efficient gene knockout screens to be added as an important orthogonal method to knockdown and chemical screens. Importantly, all of these screens are being performed in increasingly larger numbers of established and newly developed cancer cell lines, thus increasing the power to find genuine associations between gene dependen-

cies and genomic alterations. As new resources and analysis methods emerge, it will be important to further validate findings such as acute *MAP2K1* dependence in *MAP2K1*-mutant cells. Our data suggest that patients with *MAP2K1*-mutant tumors could benefit from treatment with MEK1 inhibitors, such as the approved drug trametinib, and we hope that this strategy is evaluated in a clinical setting.

Disclosure of Potential Conflicts of Interest

M. Meyerson receives research support from Bayer Pharmaceuticals. W.C. Hahn is a consultant for Novartis and Blueprint Medicines. No potential conflicts of interest were disclosed by the other authors.

Authors' Contributions

Conception and design: H.S. Gannon, N. Kaplan, M. Meyerson
Development of methodology: H.S. Gannon, N. Kaplan, A. Tsherniak
Acquisition of data (provided animals, acquired and managed patients, provided facilities, etc.): H.S. Gannon, N. Kaplan, F. Vazquez
Analysis and interpretation of data (e.g., statistical analysis, biostatistics, computational analysis): H.S. Gannon, F. Vazquez, B.A. Weir, W.C. Hahn
Writing, review, and/or revision of the manuscript: H.S. Gannon, A. Tsherniak, F. Vazquez, B.A. Weir, W.C. Hahn, M. Meyerson
Administrative, technical, or material support (i.e., reporting or organizing data, constructing databases): H.S. Gannon, N. Kaplan, A. Tsherniak
Study supervision: W.C. Hahn, M. Meyerson

Acknowledgments

The authors thank A. Ramachandran, S. Bullman, D. Cai, P. Choi, W. Lin, A. Taylor, H. Watanabe, and X. Zhang for helpful discussion during the course of this work and in article preparation.

Grant Support

This work was supported by the NIH (F32 CA196141, U01 CA176058, NCI 1R35 CA197568, and DOD W81XWH-12-1-0269) and the American Cancer Society Research Professorship.

The costs of publication of this article were defrayed in part by the payment of page charges. This article must therefore be hereby marked *advertisement* in accordance with 18 U.S.C. Section 1734 solely to indicate this fact.

Received July 22, 2015; revised October 12, 2015; accepted October 30, 2015; published OnlineFirst November 18, 2015.

References

- Druker BJ, Talpaz M, Resta DJ, Peng B, Buchdunger E, Ford JM, et al. Efficacy and safety of a specific inhibitor of the BCR-ABL tyrosine kinase in chronic myeloid leukemia. *N Engl J Med* 2001; 344:1031-7.
- Early Breast Cancer Trialists' Collaborative Group (EBCTCG). Relevance of breast cancer hormone receptors and other factors to the efficacy of adjuvant tamoxifen: Patient-level meta-analysis of randomised trials. *Lancet* 2011;378:771-84.
- Iyer G, Hanrahan AJ, Milowsky MI, Al-Ahmadie H, Scott SN, Janakiraman M, et al. Genome sequencing identifies a basis for everolimus sensitivity. *Science* 2012;338:221.
- Wagle N, Grabiner B, Van Allen EM, Hodis E, Jacobus S, Supko JG, et al. Activating mTOR mutations in a patient with an extraordinary response on a Phase I trial of everolimus and pazopanib. *Cancer Discov* 2014;4:546-53.
- Imielinski M, Greulich H, Kaplan B, Araujo L, Amann J, Horn L, et al. Oncogenic and sorafenib-sensitive ARAF mutations in lung adenocarcinoma. *J Clin Invest* 2014;124:1582-6.
- Barretina J, Caponigro G, Stransky N, Venkatesan K, Margolin AA, Kim S, et al. The Cancer Cell Line Encyclopedia enables predictive modelling of anticancer drug sensitivity. *Nature* 2012; 483:603-7.
- Forbes SA, Beare D, Gunasekaran P, Leung K, Bindal N, Boutselakis H, et al. COSMIC: exploring the world's knowledge of somatic mutations in human cancer. *Nucleic Acids Res* 2014;43(D1):D805-11.
- Cowley GS, Weir BA, Vazquez F, Tamayo P, Scott JA, Rusin S, et al. Parallel genome-scale loss of function screens in 216 cancer cell lines for the identification of context-specific genetic dependencies. *Sci Data* 2014;1: 140035 doi: 10.1038/sdata.2014.35.
- Shao DD, Tsherniak A, Gopal S, Weir BA, Tamayo P, Stransky N, et al. ATARIS: computational quantification of gene suppression phenotypes from multisample RNAi screens. *Genome Res* 2013;23: 665-78.
- Shalem O, Sanjana NE, Hartenian E, Shi X, Scott DA, Mikkelsen TS, et al. Genome-scale CRISPR-Cas9 knockout screening in human cells. *Science* 2014;343:84-7.
- Sanjana NE, Shalem O, Zhang F. Improved vectors and genome-wide libraries for CRISPR screening. *Nat Methods* 2014;11:783-4.
- Clark GJ, Cox AD, Graham SM, Der CJ. Biological assays for Ras transformation. *Methods Enzymol* 1995;255:395-412.
- Arcila ME, Drilon A, Sylvester BE, Lovly CM, Borsu L, Reva B, et al. *MAP2K1* (MEK1) mutations define a distinct subset of lung adenocarcinoma associated with smoking. *Clin Cancer Res* 2015;21: 1935-43.

14. Imielinski M, Berger AH, Hammerman PS, Hernandez B, Pugh TJ, Hodis E, et al. Mapping the hallmarks of lung adenocarcinoma with massively parallel sequencing. *Cell* 2012;150:1107–20.
15. The Cancer Genome Atlas. 2014. Comprehensive molecular profiling of lung adenocarcinoma. *Nature* 2014;511:543–50.
16. Downward J. Targeting RAS signalling pathways in cancer therapy. *Nat Rev Cancer* 2003;3:11–22.
17. Lawrence MS, Stojanov P, Mermel CH, Robinson JT, Garraway LA, Golub TR, et al. Discovery and saturation analysis of cancer genes across 21 tumour types. *Nature* 2014;505:495–501.
18. Nikolaev SI, Rimoldi D, Iseli C, Valsesia A, Robyr D, Gehrig C, et al. Exome sequencing identifies recurrent somatic MAP2K1 and MAP2K2 mutations in melanoma. *Nat Genet* 2011;44:133–9.
19. Choi YL, Soda M, Ueno T, Hamada T, Haruta H, Yamato A, et al. Oncogenic MAP2K1 mutations in human epithelial tumors. *Carcinogenesis* 2012;33:956–61.
20. Nelson DS, Van Halteren A, Quispel WT, Van Den Bos C, Bovée JV, Patel B, et al. MAP2K1 and MAP3K1 mutations in Langerhans cell histiocytosis. *Genes Chromosomes Cancer* 2015;54:361–8.
21. Chakraborty R, Hampton OA, Shen X, Simko SJ, Shih A, Abhyankar H, et al. Mutually exclusive recurrent somatic mutations in MAP2K1 and BRAF support a central role for ERK activation in LCH pathogenesis. *Blood* 2014;124:3007–15.
22. Waterfall JJ, Arons E, Walker RL, Pineda M, Roth L, Killian JK, et al. High prevalence of MAP2K1 mutations in variant and IGHV4-34 expressing hairy-cell leukemia. *Nat Genet* 2014;46:8–10.
23. Marks JL, Gong Y, Chitale D, Golas B, McLellan MD, Kasai Y, et al. Novel MEK1 mutation identified by mutational analysis of epidermal growth factor receptor signaling pathway genes in lung adenocarcinoma. *Cancer Res* 2008;68:5524–8.
24. Adjei AA, Cohen RB, Franklin W, Morris C, Wilson D, Molina JR, et al. Phase I pharmacokinetic and pharmacodynamic study of the oral, small-molecule mitogen-activated protein kinase kinase 1/2 inhibitor AZD6244 (ARRY-142886) in patients with advanced cancers. *J Clin Oncol* 2008;26:2139–46.
25. Infante JR, Fecher LA, Falchook GS, Nallapareddy S, Gordon MS, Becerra C, et al. Safety, pharmacokinetic, pharmacodynamic, and efficacy data for the oral MEK inhibitor trametinib: A phase 1 dose-escalation trial. *Lancet Oncol* 2012;13:773–81.
26. Mullard A. NCI-MATCH trial pushes cancer umbrella trial paradigm. *Nat Rev Drug Discov* 2015;14:513–5.
27. Cho J, Bass AJ, Lawrence MS, Cibulskis K, Cho A, Lee S-N, et al. Colon cancer-derived oncogenic EGFR G724S mutant identified by whole genome sequence analysis is dependent on asymmetric dimerization and sensitive to cetuximab. *Mol Cancer* 2014;13:141.
28. Caunt CJ, Sale MJ, Smith PD, Cook SJ. MEK1 and MEK2 inhibitors and cancer therapy: the long and winding road. *Nat Rev Cancer* 2015;15:577–92.
29. Wagle N, Berger MF, Davis MJ, Blumenstiel B, De Felice M, Pochanard P, et al. High-throughput detection of actionable genomic alterations in clinical tumor samples by targeted, massively parallel sequencing. *Cancer Discov* 2012;2:82–93.
30. Cheng DT, Mitchell TN, Zehir A, Shah RH, Benayed R, Syed A, et al. Memorial sloan kettering-integrated mutation profiling of actionable cancer targets (MSK-IMPACT). *J Mol Diagn* 2015;17:251–64.
31. Crystal AS, Shaw AT, Sequist LV, Friboulet L, Niederst MJ, Lockerman EL, et al. Patient-derived models of acquired resistance can identify effective drug combinations for cancer. *Science* 2014;346:1480–6.
32. Grisham RN, Sylvester BE, Won H, McDermott G, DeLair D, Ramirez R, et al. Extreme outlier analysis identifies occult mitogen-activated protein kinase pathway mutations in patients with low-grade serous ovarian cancer. *J Clin Oncol*. 2015 Aug 31. [Epub ahead of print].

Molecular Cancer Research

Identification of an "Exceptional Responder" Cell Line to MEK1 Inhibition: Clinical Implications for MEK-Targeted Therapy

Hugh S. Gannon, Nathan Kaplan, Aviad Tsherniak, et al.

Mol Cancer Res 2016;14:207-215. Published OnlineFirst November 18, 2015.

Updated version Access the most recent version of this article at:
doi:[10.1158/1541-7786.MCR-15-0321](https://doi.org/10.1158/1541-7786.MCR-15-0321)

Supplementary Material Access the most recent supplemental material at:
<http://mcr.aacrjournals.org/content/suppl/2015/12/15/1541-7786.MCR-15-0321.DC1>

Cited articles This article cites 30 articles, 10 of which you can access for free at:
<http://mcr.aacrjournals.org/content/14/2/207.full#ref-list-1>

Citing articles This article has been cited by 4 HighWire-hosted articles. Access the articles at:
<http://mcr.aacrjournals.org/content/14/2/207.full#related-urls>

E-mail alerts [Sign up to receive free email-alerts](#) related to this article or journal.

Reprints and Subscriptions To order reprints of this article or to subscribe to the journal, contact the AACR Publications Department at pubs@aacr.org.

Permissions To request permission to re-use all or part of this article, use this link
<http://mcr.aacrjournals.org/content/14/2/207>.
Click on "Request Permissions" which will take you to the Copyright Clearance Center's (CCC) Rightslink site.